

Supporting Information

A novel one-step synthesis of PEG passivated multicolour fluorescent carbon dots for potential biolabeling application

*Abhay Sachdev, Ishita Matai, S. Uday Kumar, Bharat Bhushan, Poornima Dubey and P.Gopinath**

*Nanobiotechnology Laboratory, Centre for Nanotechnology,
Indian Institute of Technology Roorkee, Roorkee, Uttarakhand-247667, India.*

Fax: +91-1332-273560;

Tel: 91-1332-285650;

E-mail: pgopifnt@iitr.ernet.in, genegopi@gmail.com

1. Experimental Section

1.1 Materials and Methods

All the chemicals were of analytical grade and used without any modification. Chitosan and PEG-4000 were purchased from Sisco Research Laboratories (SRL), India. Sulphuric acid (98%) was purchased from SD fine chemicals, India. Bacterial Growth media such as Luria-Bertani (LB) medium, Nutrient broth (NB) and ampicillin were purchased from Merck (Germany), Himedia and SRL (India), respectively. Milli-Q water (Millipore) was used for all the preparations.

1.2. Synthesis of Carbon dots

The PEG-4000 passivated fluorescent c-dots were synthesized by one-step microwave method. In a typical synthesis, 0.2 g of chitosan was added to solution containing 25 mL of water and 4 mL of concentrated H_2SO_4 . Immediately 0.2 g of PEG-4000 was added followed by intense stirring for 15 minutes. The solution was then subjected to microwave irradiation using a domestic microwave oven (IFB) operating at 100 % power level (700 W) for different cyclic times (20 s on, 10 s off). The solution was then allowed to cool naturally to room temperature and the obtained dark brown solution was centrifuged at 14000 rpm for 15 minutes to separate the less fluorogenic, insoluble black deposit from fluorogenic, yellowish brown supernatant. The supernatant containing the surface passivated C-dots was referred to as CPs. Similarly, non-passivated C-dots were synthesized by a similar scheme but without PEG-4000 and the resulting supernatant was referred to as CDs.

1.3 Effect of Microwave irradiation

The effect of microwave irradiation on absorbance and fluorescence intensity was evaluated by subjecting the solution to microwave irradiation for varying time periods.

1.4 Photostability Test

Photostability test of CPs was conducted inside a fluorescence spectrophotometer (Hitachi F-4600, Japan) equipped with Xenon arc lamp at an emission wavelength of 450 nm with time scan of 1800 s. The excitation slit width and emission slit width being 2.5 nm and 5.0 nm respectively.

1.5 Quantum Yield Measurements

A single point method was used to calculate the quantum yield of the samples using quinine sulphate as reference having quantum yield of 0.54 at 360 nm according to previously reported method [1]. The following equation was used to calculate the quantum yield

$$Q = Q_R \times \frac{I}{I_R} \times \frac{A_R}{A} \times \frac{n^2}{n_R^2}$$

where Q refers to the quantum yield of the sample, I being the measured integrated emission intensity (area under the curve), refractive index being n and A as the optical density, respectively. The subscript R refers to the reference fluorophore of known quantum yield. To minimize re-absorption effects, the absorption in the 10 mm fluorescence cuvette was kept below 0.1 at the excitation wavelength. An excitation slit width of 1.0 nm and emission slit width of 2.5 nm was used to excite the samples and record their fluorescence spectra in the wavelength range of 375-700 nm, respectively.

1.6 Bacterial Labeling Studies

To assess the bacterial labeling ability, overnight grown culture of Gram positive *S.aureus* (MTCC 737) obtained from IMTECH, India and Gram negative recombinant GFP expressing *E.coli* were chosen as model systems. For both the systems, CPs were administered (0.1mg/mL) to similar concentration of bacterial cells i.e. 10^8 CFU/mL (Optical density of 0.5 at 600 nm). All the samples were incubated at 37 °C at 220 rpm for 3 hours under stirring conditions using sterile microcentrifuge tubes. This was followed by centrifugation of the samples as well as controls at 10000 rpm for 4 minutes and then washed twice before re-suspending the pellet in 300 μ L of sterile distilled water. 5 μ L of the samples were deposited on glass slides and allowed to air dry for fluorescence microscope imaging. Similarly, time dependent bacterial labeling was studied in order to optimize the labeling time.

2. Characterization Techniques

Absorption and Fluorescence measurements were carried out using a UV-vis double beam spectrophotometer (Lasany, LI-2800) and a Fluorescence spectrophotometer (Hitachi F-4600, Japan). All the samples were diluted 10 folds for measurements. Transmission electron

microscope (TEM) analysis was performed using a FEI TECHNAI G2 and JEOL 2100 UHR-TEM operating at 200 keV by drop casting 10-20 μL sample onto non-shining side of carbon-coated copper TEM grids and were subsequently air dried. The particle diameter was estimated using ImageJ software. TEM electron dispersive X-ray study (EDX) was performed using copper grids (Sigma-Aldrich, G4901). Surface topology of the samples was analyzed by Atomic force microscope (NTEGRA PNL) operating in semi-contact mode. The images were processed using NOVA software. Field emission-scanning electron microscope (FE-SEM) operating at an accelerating voltage of 20 keV was used for morphological analysis. X-ray diffraction (XRD) patterns were obtained by Bruker AXS D8 Advance powder X-ray diffractometer (Cu-K_α radiation, $\lambda = 1.5406 \text{ \AA}$) in the range of $10-90^\circ$ at a scan speed of $0.05^\circ/\text{min}$. Fourier Transform Infrared spectroscopic (FTIR) analysis was done using a Thermo Nicolet spectrometer using KBr pellets in the range $4000-400 \text{ cm}^{-1}$. Fluorescence microscopic images were acquired using a Nikon Eclipse LV100 microscope by air drying a drop of the diluted samples on a glass slide under various excitation filters such as UV-2A (330-380 nm), B-2A (450-490 nm) and G-2A (510-560 nm) filter excitation. All images were taken at 100X magnification.

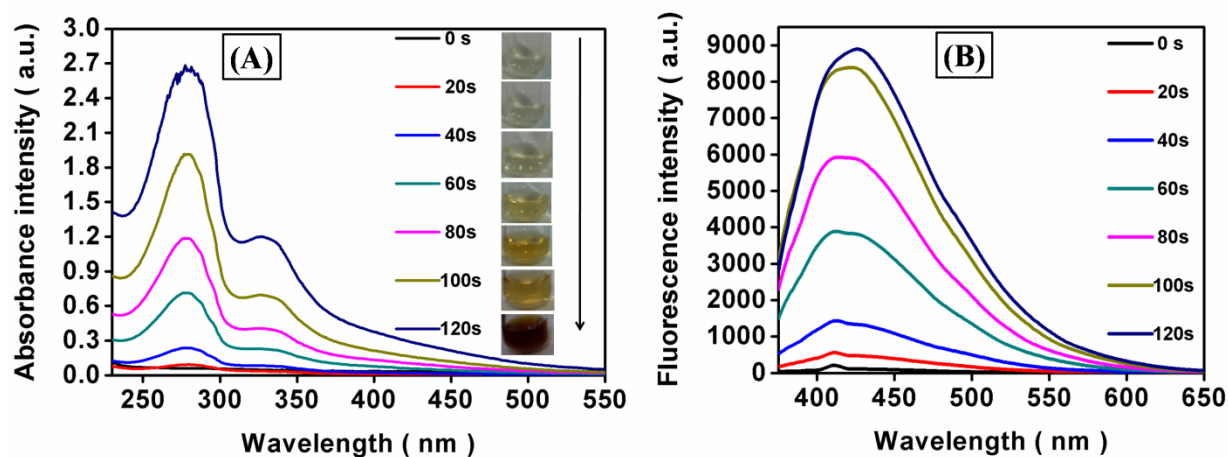


Figure S1. (A) UV-vis absorbance spectra (B) Emission spectra (excited at 360 nm) of CPs prepared at different microwave irradiation times. The inset (A) represents the photograph of as-prepared CPs.

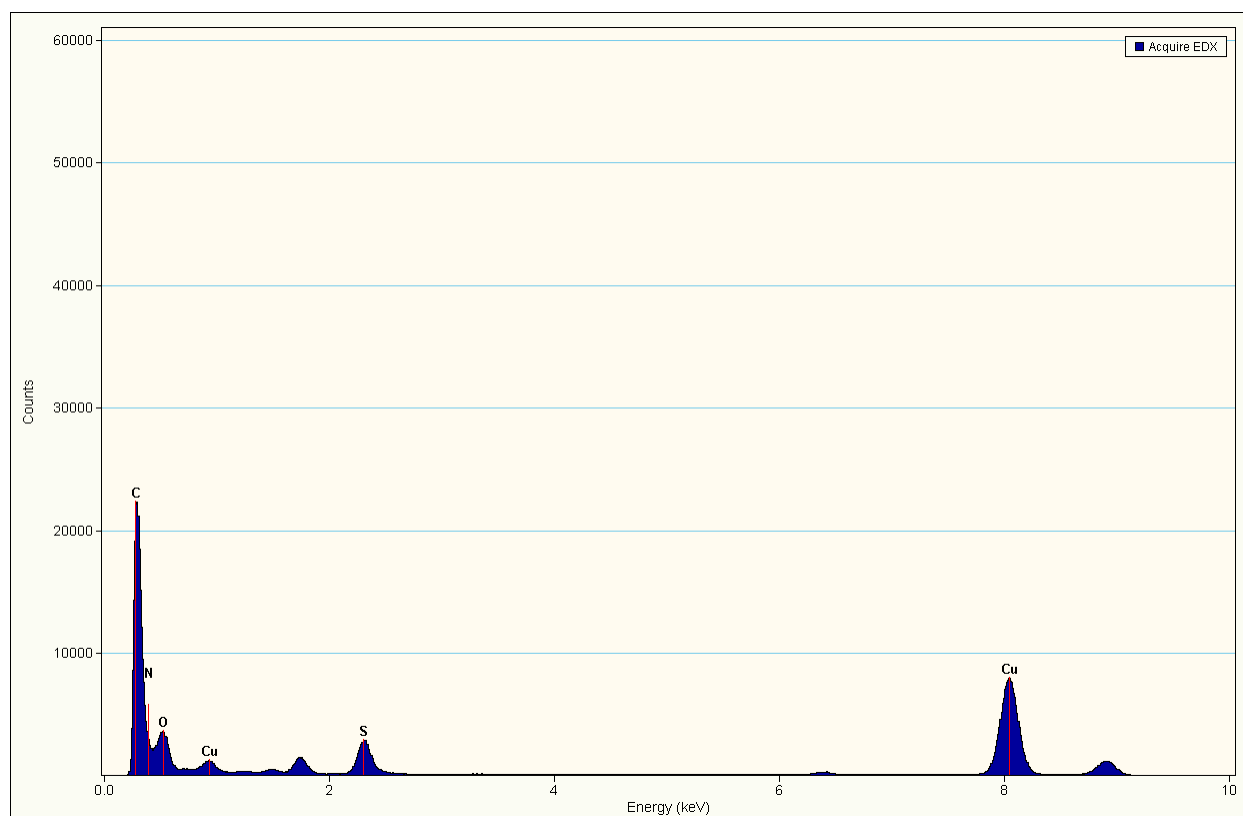


Figure S2. EDX spectrum of CPs.

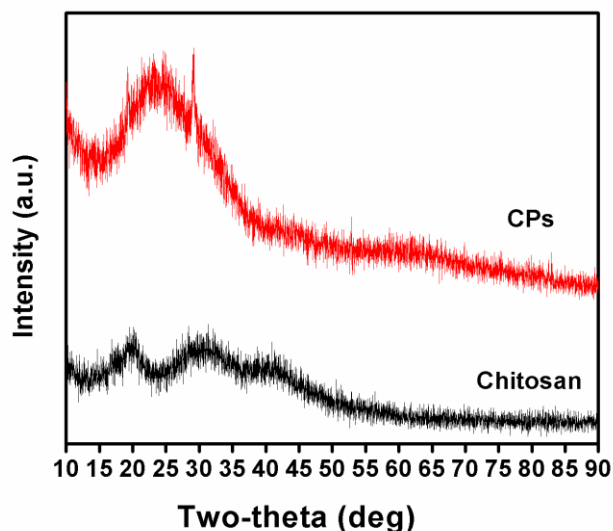


Figure S3. XRD patterns of Chitosan and CPs.

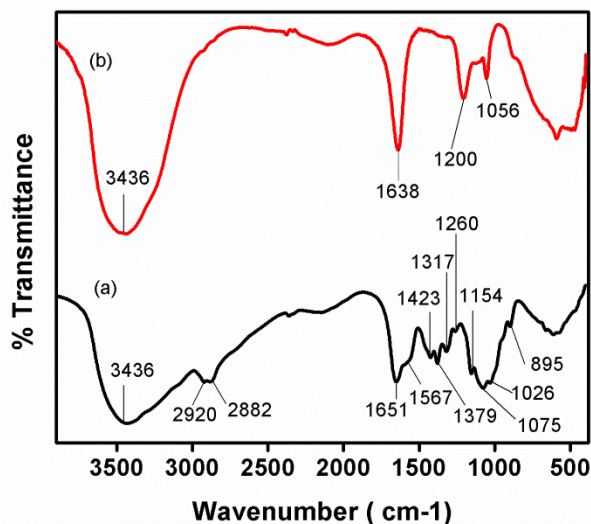


Figure S4. FTIR spectra of Chitosan (a) and CPs (b). Chitosan represents a characteristic overlapping absorption band of O-H and N-H at 3436 cm^{-1} as well as C-H stretching vibrations of CH_2 and CH_3 at 2920 cm^{-1} and 2882 cm^{-1} respectively. The stretching vibration peak at 1651 cm^{-1} corresponds to amide I ($\text{C}=\text{O}$) and bending peak at 1567 cm^{-1} corresponds to amide II (N-H), which are typical of a chitosan saccharide structure. The absorption bands at 1154 cm^{-1} and 895 cm^{-1} signify glycosidic linkages. Peaks at 1026 cm^{-1} , 1075 cm^{-1} are due to C-O stretching vibration and absorption peaks at 1379 cm^{-1} , 1423 cm^{-1} are ascribed to $-\text{CH}_3$ symmetrical deformation mode in chitosan. Additionally, the sharp peaks at 1317 cm^{-1} and 1260 cm^{-1} , are the

characteristic amine I and II C–N bonds, respectively. For CPs, the peaks at 1056 cm⁻¹ and 1200 cm⁻¹ arise due to symmetrical vibration of SO₃⁻ and C–O–C groups respectively.

Sample	Integrated emission intensity (<i>I</i>)	Absorbance at 360nm (<i>A</i>)	Refractive index of solvent(<i>n</i>)	Quantum yield at 360nm (<i>Q</i>)
Quinine sulphate	273806	0.0646	1.33	0.54 (known)
CPs	22717	0.0589	1.35	0.0506
CDs	15110	0.0591	1.35	0.0335

Table S1 Quantum yield of CPs and CDs.

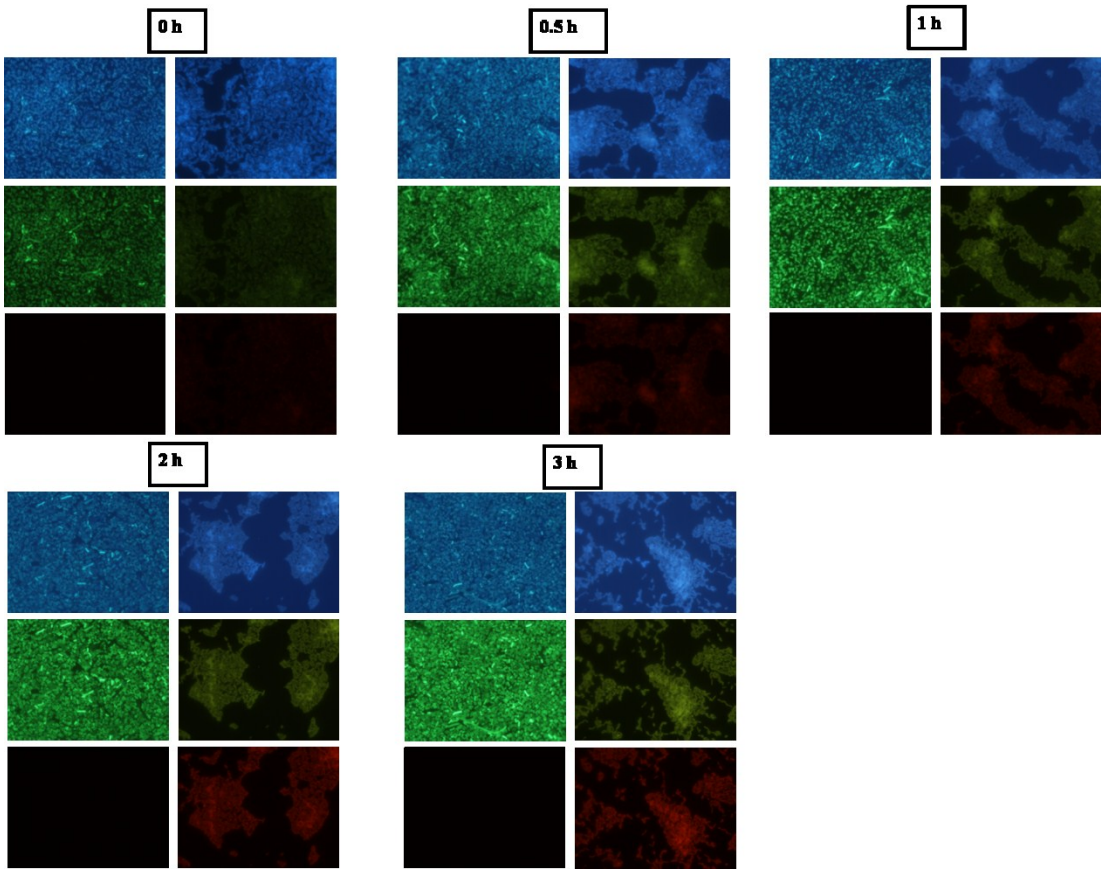


Figure S5. Fluorescence microscopic images of CPs labeled GFP *E. coli* at various time points.

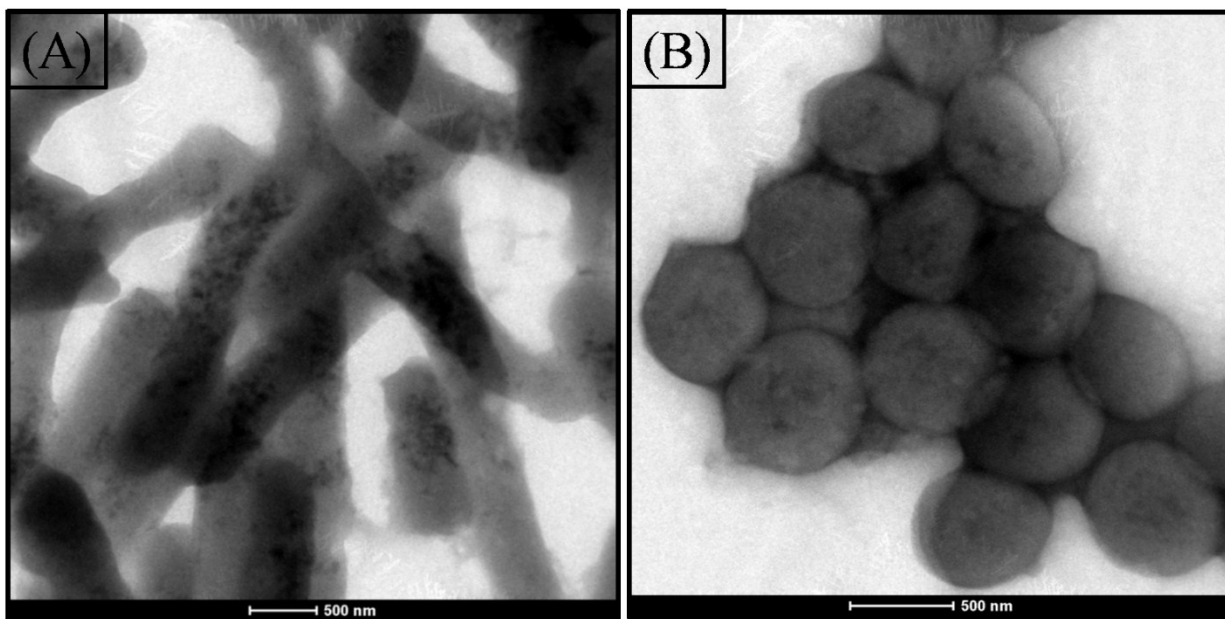


Figure S6. TEM images of (A) CPs labeled GFP *E.coli* (B) CPs labeled *S.aureus*

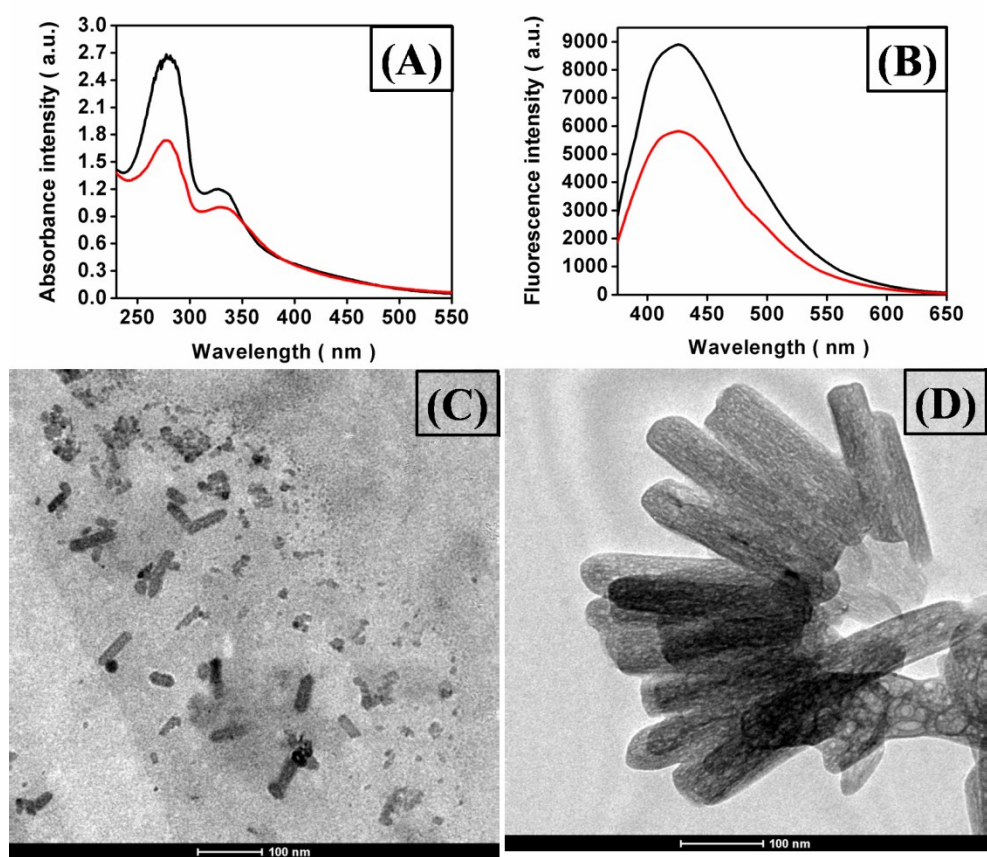
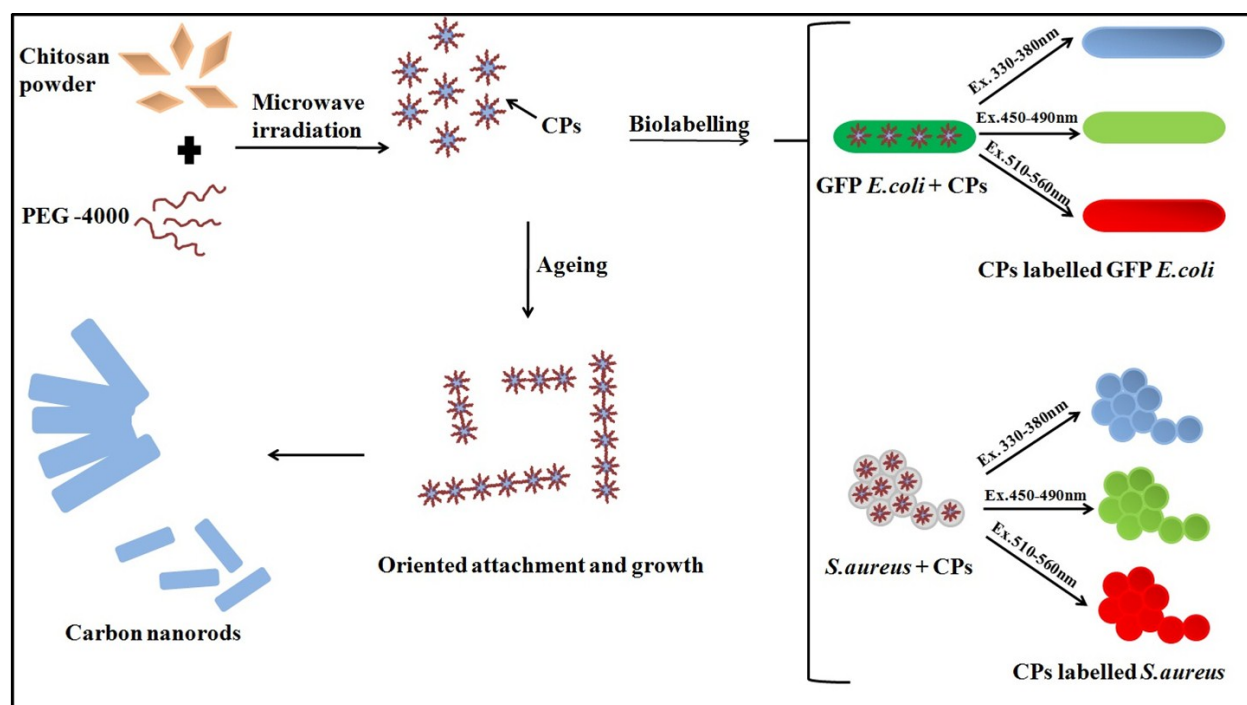


Figure S7. (A) UV-vis and (B) Emission spectra (excited at 360 nm) of fresh (black) and aged (red) CPs. (C,D) TEM images of aged CPs.



Scheme 1. One-step synthesis of multicolor CPs for biolabeling application and elucidation of the underlying mechanism.